THE ASTROPHYSICAL JOURNAL, 365:419–431, 1990 December 20

THE KINETIC EVOLUTION AND VELOCITY DISTRIBUTION OF GRAVITATIONAL GALAXY CLUSTERING

WILLIAM C. SASLAW
Department of Astronomy, University of Virginia, Institute of Astronomy, Cambridge, and National Radio Astronomy Observatory[1]
S. M. CHITRE[2]
Department of Astronomy, University of Virginia, and Institute of Astronomy, Cambridge
AND
MAKOTO ITOH AND SHOGO INAGAKI
Department of Astronomy, Kyoto University
Received 1990 April 20; accepted 1990 June 20

ABSTRACT

We derive the spatial statistical distribution function for quasi-equilibrium gravitational clustering in an expanding universe from more general assumptions than before, without needing an earlier *Ansatz*. Then we show how this statistical distribution is related to the kinetic development of the BBGKY hierarchy and how to obtain an analytic description for the time evolution of an initial Poisson distribution. From general principles, we also derive an analytic velocity distribution function for quasi-equilibrium gravitational clustering. It has no free parameters. Comparison with N-body experiments shows excellent agreement.

Subject headings: cosmology — galaxies: clustering — galaxies: formation — gravitation — hydrodynamics

I. INTRODUCTION AND BASIC RESULTS

In seeking to understand the distribution of galaxies, it seems natural to explore the role of gravitation. As a cause of large-scale clustering, gravity is ubiquitous, efficient, and dissipative: ubiquitous in its dominance of all known intergalactic forces, efficient in changing random chaos into clusters during just one or two Hubble expansion times, and dissipative in destroying the memory of nongravitational initial conditions. These properties combine to predict unique features of gravitational clustering which may be compared with observations.

Completely objective descriptions of observations which are related to the dynamics of gravitational clustering are best suited for this comparison. Descriptions which contain more information are likely to be more useful. Correlation functions have been the most popular description. Many studies of the two-point correlation function (summarized, for example, in Peebles 1980; Saslaw 1985*a*) have shown how it can be derived theoretically from the gravitational BBGKY hierarchy in the linear regime and from thermodynamic arguments and N-body simulations in the nonlinear regime. It can be measured objectively in a system whose conditional density is homogeneous (Coleman, Pietronero, and Sanders 1988). Its information content, however, is limited and describes the galaxy distribution inadequately. If all the higher order correlation functions were known, they would provide a complete description of the distribution. Even at the level of the three-point correlation function, however, they become very difficult to measure accurately and cannot be calculated dynamically from first principles, even in the linear regime, without powerful constraining assumptions. Other recent objective measures of clustering, such as its fractal nature (e.g., Pietronero 1987) or its topology (e.g., Gott *et al.* 1989), contain more information with different emphases than the two-point correlation function. These promising new descriptions are still insufficiently related to the underlying dynamics, although N-body simulations have provided very useful experimental examples.

In this paper we examine an objective description of clustering, which contains much more information than the low-order correlation functions, which can be derived theoretically from gravitational dynamics, and which can be measured easily: the distribution function. Historically, this is the oldest measure of galaxy clustering, having been used by Herschel (1785), who speculated on its gravitational origin long before anyone understood the nature of the nebulae. The full distribution function $f(N, v)$ is just the probability that a region of a given volume, V, or of a given area on the sky contains N galaxies with peculiar velocities (relative to the Hubble expansion) between v and $v + dv$. This does not contain complete information about the individual positions and velocities of each galaxy; it is a statistical description at the same level as the Maxwell-Boltzmann distribution for a perfect gas. We are interested here in the gravitational analogue of the Maxwell-Boltzmann distribution for a system of interacting galaxies in the expanding universe.

Most previous work on $f(N, v)$ has been concerned with the spatial distribution function of galaxies, $f(N) = \int f(N, v)dv$. Under certain assumptions, to be discussed shortly, the theory of gravitational clustering predicted (Saslaw and Hamilton 1984) that

$$f(N) = \frac{\bar{N}(1-b)}{N!}\,[\bar{N}(1-b) + Nb]^{N-1} e^{-\bar{N}(1-b)-Nb}\,, \tag{1}$$

[1] Operated by Associated Universities, Inc., under cooperative agreement with the National Science Foundation.
[2] On leave of absence from TIFR, Bombay.

where

$$\bar{N} = \bar{n}V \tag{2}$$

is the expected number of galaxies in a volume V for average number density $\bar{n}$, and

$$b = -\frac{W}{2K} = \frac{2\pi G m^2 n}{3T} \int_0^\infty \xi(n, T, r) r \, dr \tag{3}$$

is the ratio of gravitational correlation energy to the kinetic energy of peculiar velocities. Here ξ is the two-point correlation function, which may generally contain a time-dependent scale length, and

$$K = \tfrac{3}{2}NT = \tfrac{1}{2}\sum_{i=1}^{N} m v_i^2 \tag{4}$$

is the kinetic energy of peculiar motions of the N galaxies in the volume V. Subsequently, this distribution was found to give a good description of galaxies in the Zwicky catalog (where the value of $b = 0.70 \pm 0.05$; Crane and Saslaw 1986), of the galaxies in the *CfA* slice (where the value of b is also 0.7; Crane and Saslaw 1988), of the Abell clusters (for which $b = 0.3 \pm 0.1$; Coleman and Saslaw 1990), and of N-body simulations for a range of initial conditions, masses, and values of Ω_0 (Saslaw and Hamilton 1984; Saslaw 1985*b*; Itoh *et al.* 1988, 1990). When gravity is ineffective, $b = 0$ and $f(N)$ reduces to a Poisson distribution which has the Maxwell-Boltzmann form in the limit of large N.

We now extend this approach by: (*a*) strengthening the thermodynamic derivation of equation (1), showing that a major assumption used previously is not needed but follows from more fundamental properties; (*b*) deriving the early kinetic nonequilibrium evolution of the gravitational distribution, showing how it makes a transition from a Poisson distribution with $b = 0$ (a Maxwell-Boltzmann "gas") to a distribution of the form of equation (1) with nonzero b; and (*c*) obtaining the velocity distribution $f(v)$ consistent with equation (1), comparing it with N-body simulations and with properties of the gravitational Fokker-Planck equation. These are the basic results of §§ II–IV. To help put our new results in perspective, we next discuss the assumptions which led to the derivation of equation (1).

Assumptions used to derive equation (1) describe either general properties of the distribution or constitutive properties of the system. The general assumptions, which could be true of many distributions, are statistical homogeneity and scale invariance. The constitutive assumptions, which apply specifically to the gravitational interaction and cosmological conditions, are the pairwise interaction of galaxies as mass points, the quasi-equilibrium evolution of the distribution, and the particular form of $b(n, T)$. This last assumption was originally an independent *Ansatz* of the theory, based on mathematical simplicity. We now show, in § II, that the same form of $b(n, T)$ assumed originally can be determined uniquely by more fundamental properties of the theory, thus removing it as an independent *Ansatz*. First, we comment on each of these assumptions in turn.

Statistical homogeneity requires that $f(N)$ and $f(N, v)$ measured using any large number of volumes will be independent (within the noise uncertainty) of which volumes are actually sampled. That is to say, any sufficiently large number of volumes provides a "fair sample." These volumes may be drawn from an ensemble of statistically independent (uncorrelated) microscopic realizations of the macroscopic systems, if available. In the case of our universe, with only one system available to measure, we must assume that samples can be drawn from statistically independent regions, which are not connected by large-scale structures. These regions may, however, contain large-scale correlations, provided that every point or galaxy is equivalent with regard to these correlations. In other words, all the correlation functions depend only on relative positions, not on absolute coordinates. Statistical homogeneity may exist on some scales, but not on others. It can be a property of an infinite or unbounded gravitating system, but not of a finite bounded one.

Scale invariance may apply to volumes over which homogeneity exists. On these scales, the value of b is independent of scale: $b(\lambda r) = b(r)$ with λ, a scalar multiple. Equation (1) was originally derived with the idealized assumption that scale invariance holds on all scales. Although this will not rigorously apply to a kinetic system in which the correlation length scale increases with time, the N-body simulations (Itoh *et al.* 1988) show that scale invariance applies for a wide range of conditions to those scales which have had time to relax, and equation (1) is adequately satisfied. Scale-free initial conditions relax most rapidly, especially for larger values of the cosmic density parameter, Ω_0, but even structured initial conditions are gradually dissipated on increasing scales. These results do not depend strongly on the masses of the galaxies (Saslaw 1985*b*; Itoh *et al.* 1990), since most of the later relaxation arises from collective interactions.

Pairwise gravitational interaction of galaxies as point masses is a constitutive assumption which helps define the specific properties of galaxy clustering. It applies if most of the clustering occurs after galaxies have become well-defined dynamical entities separated by distances much greater than their individual sizes. (A small fraction of colliding or merging galaxies, however, will not affect these statistics significantly.) The pairwise interaction leads to a specific form of the equation of state (Saslaw and Hamilton 1984) in which the internal energy, U, and pressure, P, are linear functions of b which depend directly on only the two-point correlation function. Thermodynamic quantities can then be defined in a system, or an ensemble of systems, over scales which are statistically homogeneous and scale invariant. They can also be generalized for systems where these properties vary slowly over the entire system (Saslaw 1989).

Quasi-equilibrium evolution may seem, at first sight, to be an unpromising assumption. We know that Newtonian point gravitating systems have no rigorous equilibrium state since the gravitational force does not saturate. Quasi-equilibrium evolution, which takes place through a sequence of equilibrium states whose properties change with time, is the next most simple description. It occurs, in the context of galaxy clustering, essentially because the expansion of the universe implicitly removes the effect of the mean gravitational field and inhibits the growth of gravitational instabilities. This is a situation where we can turn the lack of an

exponentially growing Jeans instability (a disadvantage for galaxy formation) to an advantage for obtaining a theoretical description of galaxy clustering. Computer N-body experiments confirm the applicability of the idea of quasi-equilibrium evolution to galaxy clustering (Itoh *et al.* 1988), and theoretical arguments (Saslaw 1986; Zhan 1989; Zhan and Dyer 1989) support it further. The relaxation processes which drive the clustering through these quasi-equilibrium states are quite different from the hard collisions familiar in the case of a perfect atomic gas. Evolution from a Poisson initial state begins with the large mutual deflections of near neighbors to form small groups, followed by the collective interactions of these small groups to form larger groups and clusters. Larger length scales tend to cluster on longer time scales. After a short transition period of one or two Hubble expansion time scales, $f(N)$ is described by equation (1) with $b(t)$ changing more slowly than the Hubble expansion. Since $b(t)$ [along with the average number density $\bar{n}(t)$, whose change amounts to just a renormalization of $f(\bar{N})$] describes the changing thermodynamic properties of the system, these properties can evolve consistently in a quasi-equilibrium manner.

Even for some cases of unrelaxed, nonequilibrium gravitational clustering, numerical experiments (Suto, Itoh, and Inagaki 1990) show that equation (1) can still describe the distribution, provided that b is allowed to vary with scale. This is analogous to ordinary nonequilibrium thermodynamics in which macroscopic thermodynamic parameters such as temperature, pressure, and density are allowed to vary with position.

A particular form of $b(n, T)$ must be specified in order to calculate the complete gravitational equation of state which is then combined with thermodynamic fluctuation theory to derive equation (1). The assumption of scale invariance implies (Saslaw and Hamilton 1984) that b depends on the density and temperature only in the combination $G^3m^6nT^{-3}$. To obtain a more specific form of $b(nT^{-3})$, Saslaw and Hamilton (1984) assumed the simplest mathematical form which has the expected physical limits of $b = 0$ for a perfect gas and $b = 1$ for a hierarchical system dominated by gravity in virial equilibrium on all scales. This suggested the *Ansatz*

$$b = \frac{b_0 nT^{-3}}{1 + b_0 nT^{-3}}, \tag{5}$$

where b_0 is a positive constant which does not need to be specified to obtain equation (1). Originally, this was regarded as a first approximation to which additional terms might be added to find a more accurate form of $f(N)$ than equation (1). The rather extraordinary agreement of equation (1) with the N-body simulations in the applicable relaxation range, and with the observed galaxy distribution, however, leads to the expectation that it might be based on more fundamenal considerations. We show, in § II, that this is indeed the case. If initial correlations on very large scales are small and do not have time to grow significantly, $f(N)$ should have a Poisson form for these very large volumes. Nearly any modification of equation (5) would cause the $f(N)$ distribution function to diverge from this Poisson limit.

It also becomes possible (§ III) to understand how the form of equation (1) arises kinetically out of an initial Poisson distribution. From the relation between the low-order correlation functions and the generating function of $f(N)$, we obtain the early evolution of $f(N)$ for small values of b. The form of equation (1) implies that Q_3, the coefficient of the three-point correlation function, has a value of $\frac{3}{4}$, in reasonable agreement with its observed value.

Nearly all theoretical work so far has been concerned with the spatial gravitational $f(N)$ distribution. In the present work, we go further to derive the velocity distribution implied by equation (1). For relaxed clustering, it has the form (§ IV)

$$f(v)dv = \frac{2\alpha^2\beta(1-b)}{\Gamma(\alpha v^2 + 1)} [\alpha\beta(1-b) + \alpha b v^2]^{\alpha v^2 - 1} e^{\alpha\beta(1-b) - \alpha b v^2} v\, dv, \tag{6}$$

where

$$\beta = \langle v^2 \rangle \tag{7}$$

is the average velocity dispersion, α is an average structure factor which satisfies

$$GmN\left\langle \frac{1}{r} \right\rangle = \alpha v^2, \tag{8}$$

and

$$\alpha\beta = Gm\left\langle \frac{1}{r} \right\rangle, \tag{9}$$

with $\langle 1/r \rangle$ being the average inverse separation of galaxies. In equation (6), velocities are scaled to natural units in which G, m, and the radius of the total system are all unity.

Comparison of equation (6) with gravitational N-body experiments shows remarkable agreement. Furthermore, we show that this velocity distribution satisfies the basic previously known forms of the dynamical friction coefficient and the stochastic force in the gravitational Fokker-Planck equation. If this velocity distribution is also observed to occur in a fair sample of galaxies, it will further strengthen the case that quasi-equilibrium gravitational evolution determines the large-scale distribution of the galaxies.

II. THE UNIQUENESS OF THE THERMODYNAMIC DISTRIBUTION FUNCTION

In this Section, we will show that the thermodynamic distribution function of equation (1) follows from the assumption that, on the largest scales, the distribution has a Poisson form. This assumption, which can replace the *Ansatz* of equation (5), means that correlations on the largest scale are feeble or nonexistent. It would occur if initial large-scale correlations were small and did not have enough time to grow significantly.

a) Generalized $f(N)$ Distributions

To derive this result, we first need to calculate how $f(N)$ is generalized if we change the relation (5) between b, n, and T. The main steps in calculating $f(N)$ may be summarized as follows (Saslaw and Hamilton 1984):

1. Substitute equation (5), or a modification of it, into the general expressions for the internal energy

$$U = \tfrac{3}{2}NT(1 - 2b)\,, \tag{10}$$

and the pressure

$$P = \frac{NT}{V}(1 - b)\,, \tag{11}$$

of a pairwise interacting system.

2. Use the general thermodynamic relation $T\,dS = dU + P\,dV$ to calculate the gravitational contribution to the entropy $S(N, T, b)$.

3. Calculate the chemical potential $\mu(n, b)/T$ from the general relation

$$\frac{\mu}{T} = \frac{U}{NT} - \frac{S}{N} + \frac{\Psi}{N}$$

$$= \ln(nT^{-3/2}) - b - \int n^{-1} b\,dn\,, \tag{12}$$

where

$$\Psi = \frac{PV}{T} = N(1 - b) \tag{13}$$

is the grand canonical potential. The grand canonical ensemble is the relevant system for considering fluctuations of number and energy in different regions of the galaxy distribution.

4. Obtain the distribution function $f(N)$ from general thermodynamic fluctuation theory, which gives

$$f(N) = e^{-\Psi}\frac{e^{\mu N/T}}{N!}(e^{\Psi})_0^{(N)}\,, \tag{14}$$

with

$$(e^{\Psi})_0^{(N)} = \left[\left\{ne^{-\mu/T}\frac{db}{d[n(1 - b)]}\frac{d}{db}\right\}^N e^{Vn(1-b)}\right]^{n=0} \tag{15}$$

In the earlier investigation, this procedure was applied by adopting equation (5) to obtain the fundamental distribution of equation (1). We now explore the consequences of modifying equation (5). To do this most simply, we rewrite it in the more general form

$$n(1 - b) = \frac{\phi(b)}{b_0 T^{-3}}\,. \tag{16}$$

Previously $\phi(b) = b$ was used to give equation (1). Now we let $\phi(b)$ be an arbitrary function of b which satisfies the boundary condition

$$\phi(0) = 0\,. \tag{17}$$

This boundary condition represents the fact that in an ensemble of systems, those with $b \to 0$ represent a perfect gas for which $GT^{-1} \to 0$. Either the gravitational interactions between objects can be decreased or the thermal energy can be made very large compared to the interaction energy to obtain the perfect gas limit.

Substituting equation (16) into equation (12) gives

$$\frac{\mu}{T} = \ln[n(1 - b)T^{-3/2}] - \int\frac{b\phi'(b)}{\phi(b)}\,db\,, \tag{18}$$

which reduces to equation (38b) of Saslaw and Hamilton (1984) for $\phi(b) \propto b$ (after correcting the misprint of $+3/2$ for $-3/2$ in the exponent of T). From equation (15), we now obtain the more general forms of $(e^{\Psi})_0^{(N)}$ for any nonzero $b_0 T^{-3}$:

$$(e^{\Psi})_{b=0}^{(0)} = 1\,, \tag{19}$$

$$(e^{\Psi})_0^{(1)} = VT^{3/2}\lim_{b\to 0} e^{\int(b\phi'/\phi)db}\,, \tag{20}$$

$$(e^{\Psi})_0^{(2)} = VT^3 b_0 T^{-3}\lim_{b\to 0}\left[\left(\frac{V}{b_0 T^{-3}} + \frac{b}{\phi} + \frac{1}{\phi'}\right)e^{2\int(b\phi'/\phi)db}\right], \tag{21}$$

$$(e^{\Psi})_0^{(3)} = VT^{9/2}(b_0 T^{-3})^2\lim_{b\to 0}\left[\left\{\left[\frac{2V}{b_0 T^{-3}\phi'} + \frac{2b}{\phi\phi'} - \frac{\phi''}{(\phi')^3} + \frac{1}{\phi\phi'} - \frac{b}{\phi^2}\right]\right.\right.$$

$$\left.\left. + \left[\frac{1}{(\phi')^2} + \frac{b}{\phi\phi'} + \frac{V}{b_0 T^{-3}\phi'}\right]\left(\frac{2b}{\phi} + \frac{V}{b_0 T^{-3}}\right)\right\}e^{3\int(b\phi'/\phi)db}\right]. \tag{22}$$

We can also derive the generalized integral of the two-point correlation function from the general relation between the density variance and the grand canonical potential:

$$\langle (\Delta N)^2 \rangle = \langle (N - \bar{N})^2 \rangle = \frac{\partial^2 \Psi}{\partial^2 (\mu/T)} \bigg|_{T,V} . \tag{23}$$

Using equations (16) and (18), we obtain $\partial(\mu/T)/\partial b\,|_{T,V} = (1 - b)\phi'/\phi$, and hence

$$\langle (\Delta N)^2 \rangle = \frac{\bar{N}}{(1-b)^2} \left[1 - \frac{b\phi'(b) - \phi(b)}{\phi'(b)} \right], \tag{24}$$

which can be related to the two-point correlation function through the standard expression (e.g., Landau and Lifshiftz 1958)

$$\begin{aligned} \frac{1}{V^2} \iint \xi_{12}\, dV_1\, dV_2 &= \frac{1}{\bar{N}} \left[\frac{(\Delta N)^2}{\bar{N}} - 1 \right] \\ &= \frac{1}{\bar{N}} \left[\frac{1}{(1-b)^2} - 1 - \frac{b\phi' - \phi}{(1-b)^2 \phi'} \right]. \end{aligned} \tag{25}$$

When $\phi(b) \propto b$, as in equation (5) the expressions (19)–(25) reduce to the earlier results of Saslaw and Hamilton (1984); here we see how they are altered for general $\phi(b)$.

The uncorrelated state $\xi_{12} = 0$ corresponds to the Poisson distribution for which $b = 0$. To obtain this limiting state, we suppose that as $b \to 0$ the right-hand side becomes proportional to b^α with $\alpha > 0$. It is readily seen that, for any value of α, there are no solutions of the resulting linear differential equation for $\phi(b)$ which satisfy the boundary condition $\phi(0) = 0$ of equation (17). Therefore, the only way to obtain a consistent Poisson limit is to require $b\phi' - \phi = 0$, which implies that, in this limit, $\phi(b)$ is an analytic function for small b. Thus we may write

$$\phi(b) = b\eta(b) \tag{26}$$

with $\eta(b) = 1 + a_1 b + a_2 b^2 + \cdots$. We next find a restriction on $\eta(b)$.

b) *A More Fundamental Basis for the Original Ansatz*

In addition to the standard Poisson limit $b \to 0$, there is another limit in which the distribution function would be expected to have a form similar to a Poisson distribution. This occurs for b independent of scale when N is measured for volumes much larger than any correlation length scale. Statistical fluctuations of N from volume to volume, in this case, are essentially $N^{1/2}$ variations modified by any correlations which may cross the boundaries of the volumes. To illustrate this, we may examine the tail of $f(N)$ from equation (1) in the limit

$$N \to \infty, \qquad \bar{N} \to \infty, \qquad \frac{\bar{N} - N}{\bar{N}} \to 0 . \tag{27}$$

We see that

$$f(N) \to (1 - b) \frac{1}{N!} \bar{N}^N e^{-\bar{N}} , \tag{28}$$

so that the Poisson form, reduced by the factor $(1 - b)$, emerges again.

Any modification of $\phi(b)$ which has the general form of equation (26) leads to the modified $f(N)$ distribution

$$f_{\rm mod}(N) = \frac{e^{-\bar{N}(1-b)}}{N!} (be^{-b})^N (\eta e^{-\int b\, d \ln \eta})^N (e^{\Psi}_{\rm mod})^{(N)}_0 , \tag{29}$$

by combining equations (26), (18), and (14), along with (19)–(22) for $N = 0$–3. Since $\lim_{b \to 0} \eta = 1$, the e^{Ψ} factors will be changed only for $f(3)$ and higher $f(N)$. For $N < 3$, the only modification of $f(N)$ is the $\eta^N \exp [-N \int b\, d \ln \eta]$ factor.

It is worth noting that the fits of equation (1) to the N-body experiments (Itoh *et al.* 1988) are so close that they put stringent limits on any particular form of $\eta(b)$ one might wish to assume to obtain $f_{\rm mod}(N)$. We have found, for example, that the unmodified $f_{100}(V)$ of equation (1) provides an excellent fit to the experimental distribution.

More generally, in the limit of large N given by equation (27), the modified distribution will diverge away from the Poisson form unless $\eta = 1$. This is because the exponential factors in $e^{\Psi}_{\rm mod}$ vanish in their limit of $b = 0$ with $\eta(0) = 1$, as may be seen from equations (20)–(22). This leaves the $\exp \{-N \int b\, d \ln \eta\}$ factor in $f_{\rm mod}(N)$, which will only agree with the Poisson form if η is a constant independent of b. The constant can be normalized to unity by changing the value of b_0 [which does not affect $f(N)$], so we obtain the original *Ansatz* of equation (5). This also shows why the thermodynamic $f(N)$ would not be expected to apply to an unrelaxed system with inhomogeneous (possibly initial) correlations over all scales, for then it would not satisfy the Poisson form as N becomes arbitrarily large.

III. THE KINETIC EVOLUTION OF THE SPATIAL DISTRIBUTION FUNCTION

Having strengthened the derivation of equation (1), we next ask how $f(N)$ emerges from an initially uncorrelated distribution. How does a Poisson distribution grow a nonzero b, and evolve into the thermodynamic $f(N)$? In exploring this question, we find as

a bonus that equation (1) yields a particular value of Q_3, the coefficient of the three-particle hierarchial correlation function, and this value is consistent with the observed value.

Any $f(N)$ distribution can be presented compactly by a generating function

$$g(s) = \sum_{N=0} f(N)s^N , \tag{30}$$

where s is an arbitrary variable used as a counter, and $g(1) = 1$ since there must be some number, including zero, of galaxies in any volume. This generating function can be expressed in terms of volume integrals of the N-particle correlation functions ξ_N by the general relation (Balian and Schaeffer 1989)

$$g(s) = \exp\left[\sum_{N=1}^{\infty} \frac{\bar{n}^N(s-1)^N}{N!} \int_V d^3\mathbf{r}_1 \cdots \int_V d^3\mathbf{r}_N \, \xi_N(\mathbf{r}_1 \cdots \mathbf{r}_N)\right], \tag{31}$$

with $\xi_1 \equiv 1$.

Early evolution from an initial Poisson state is characterized by $\xi_{N>2} \ll \xi_2$ and $-W/K = 2b \ll 1$ so that to order b

$$g(s) = \exp\left[\bar{N}(s-1) + \frac{\bar{N}^2}{V^2}\frac{(s-1)^2}{2}\iint \xi_{12}\, dV_1\, dV_2\right]. \tag{32}$$

The first term of the exponential gives the generating function for a Poisson $f(N)$; the second term shows how the growing two-point correlation function modifies $f(N)$. Expanding the volume integral in terms of the ratio of correlation to kinetic clustering energy as

$$\frac{\bar{N}}{V^2}\iint \xi_{12}\, dV_1\, dV_2 = -\frac{W}{K} + O\left[\left(\frac{-W}{K}\right)^2\right] = 2b + O[(2b)^2] \tag{33}$$

during the early development (this form also follows from eq. [25]) gives

$$g(s) = e^{\bar{N}(s-1) + \bar{N}b(s-1)^2} . \tag{34}$$

Comparing equation (34) with the generating function for the gravitational $f(N)$ of equation (1), namely (Saslaw 1989)

$$g(s) = \exp\left\{-\bar{N} + \bar{N}\left[b + \frac{(1-b)}{b}\sum_{N=1}\frac{N^{N-1}}{N!}b^N e^{-Nb}s^N\right]\right\}, \tag{35}$$

shows they are the same to order b. Therefore, equation (32) describes the initial evolution of the gravitational distribution function $f(N)$ away from its Poisson state, toward the quasi-equilibrium distribution of equation (1). The specific time evolution of $b(t)$ may be calculated from the cosmic energy equation (Saslaw 1986) or from the solutions of the BBGKY hierarchy (Zhan, 1989; Zhan and Dyer 1989).

We can go further to show that the kinetic development implied by equation (31) is also consistent with the gravitational distribution of equation (35) to order b^2. For this we need the volume integral of ξ_3, which we assume has the hierarchial form

$$\xi_3 = Q_3(\xi_{12}\xi_{13} + \xi_{23}\xi_{21} + \xi_{31}\xi_{32}) . \tag{36}$$

Using equation (33), from which we need just the same first-order term which gave equation (34), we may write

$$\frac{\bar{N}^2}{V^3}\iiint \xi_3\, dV_1\, dV_2\, dV_3 = \frac{3Q_3\bar{N}^2}{V^3}\iiint \xi_{12}\xi_{13}\, dV_1\, dV_2\, dV_3$$
$$= 3Q_3(2b)^2 = 12Q_3 b^2 . \tag{37}$$

We next need the second-order extension of equation (33) to obtain the second term of equation (31) to order b^2. In fact, this second term of equation (31) is available to all orders of b from equation (25), with $b\phi' = \phi$ as required by the large N Poisson limit. Although the derivation of equation (25) uses the same basic assumptions as lead to equation (1), it does not depend on the $f(N)$ and may be viewed independently.

Substituting equations (25) and (37) into the general expression (31) and comparing with the gravitational generating function (35) shows that they are identical to order b^2, provided

$$Q_3 = \tfrac{3}{4} . \tag{38}$$

Therefore, the gravitational $f(N)$ distribution is consistent with the hierarchial three-particle correlation function for this value of Q_3. According to Peebles (1980), the observed value of Q_3 is 0.80 ± 0.07, although earlier for a different observed sample, Groth and Peebles (1977) found $Q_3 = 1.29 \pm 0.21$; it is rather difficult to extract this quantity accurately from the observations. After deriving the result (38), we learned that Zhan and Dyer (1989) had independently derived a relation between Q_3 and $f(N)$ from a complementary point of view, which gives a good numerical fit for $Q_3 = 0.73$ in the nonlinear regime, so these results appear consistent with each other and can be tested with more refined observations.

IV. THE VELOCITY DISTRIBUTION FUNCTION $f(v)$

a) Form of the Distribution

As the galaxies begin to cluster, their velocities depart from the Hubble flow and build up a gravitationally consistent distribution. A method for finding the form of this velocity distribution follows from the spatial fluctuation distribution given by equation (1).

We can derive the velocity distribution $f(v)$ in a simple manner by assuming:

1. As the system relaxes into a quasi-equilibrium state over a range of scales, the complete distribution function on those scales evolves into a separable distribution of N and v, that is

$$f(N, v) \rightarrow f(N)h(v) . \tag{39}$$

2. In quasi-equilibrium, the fluctuations in potential energy over a given volume (caused by correlations among particles) are proportional to the local kinetic energy fluctuations, so that

$$GmN\left\langle \frac{1}{r} \right\rangle = \alpha v^2 . \tag{40}$$

In equation (40), the average inverse particle separation $\langle 1/r \rangle$ is the expected value for a uniform Poisson distribution. Therefore, α represents the local correlations which depart from a uniform distribution. It may be thought of as a local "form factor" which relates the kinetic and potential energy fluctuations. Smaller values of α imply a more condensed, nonuniform region of particles with higher local velocity dispersion v^2. Generally, α will vary from volume to volume. We shall henceforth make the simplifying approximation that α has a constant value which is its average over the entire system. Computer simulations described below show that this is quite a good approximation. If we then average equation (40) over the entire system to obtain the mean square velocity dispersion $\langle v^2 \rangle$, treating each particle's peculiar velocity individually so that $\langle N \rangle = 1$, we have the relation

$$\alpha = \left\langle \frac{1}{r} \right\rangle \langle v^2 \rangle^{-1} , \tag{41}$$

in natural units with $G = m = R = 1$ (which we shall use hereafter), taking α to denote its average value.

With these assumptions, the first step to finding the velocity distribution is to rescale equation (1) from density fluctuations to kinetic energy fluctuations by replacing N with $N\langle 1/r \rangle$ and $\bar{N}$, the average number in a given size volume, with $\bar{N}\langle 1/r \rangle$. The second step is to substitute αv^2 for $N\langle 1/r \rangle$ from equation (40), recognizing that $N! = \Gamma(N + 1)$, and $\alpha\langle v^2 \rangle$ for $\bar{N}\langle 1/r \rangle$. The third step is to convert from kinetic energy fluctuations to velocity fluctuations using the Jacobian $2\alpha v$. The result is

$$f(v)dv = \frac{2\alpha^2\beta(1-b)}{\Gamma(\alpha v^2 + 1)} [\alpha\beta(1-b) + \alpha b v^2]^{\alpha v^2 - 1} e^{-\alpha\beta(1-b) - \alpha b v^2} v \, dv , \tag{42}$$

where

$$\beta = \langle v^2 \rangle \tag{43}$$

and Γ is the usual gamma function.

On the high-velocity tail of the distribution, for $\alpha v^2 \gg 1$ and $v^2 \gg \beta$, we obtain

$$f(v)dv \sim \left(\frac{2}{\pi}\right)^{1/2} \alpha^{3/2} \frac{\beta(1-b)}{b} (\alpha v^2)^{-1} (be^{1-b})^{\alpha v^2} dv . \tag{44}$$

In the limit of very high velocities, this satisfies the differential equation

$$\frac{df}{dv} = 2\alpha \ln (be^{1-b}) vf , \tag{45}$$

which we shall find to have an interesting physical interpretation in § IV*b*. Note that for the values of b of interest, $0 < b < 1$; the logarithm in equation (45) is negative, so that the high-velocity tail of $f(v)$ always behaves like a Maxwellian. However, the limit of $f(v)$ as $b \rightarrow 0$ will not be a Maxwell-Boltzmann distribution because a Maxwellian does not satisfy the relation $N \propto v^2$ of equation (40) in this limit. The Maxwell-Boltzmann limit of $f(v)$ requires both $b \rightarrow 0$ and no correlation between N and v.

b) Relation to the Fokker-Planck Equation

When gravitational clustering is very nonlinear, the galaxies will have high peculiar velocities, and they deflect the orbits of each other only slightly. Fokker-Planck equations describe this situation. We would therefore expect $f(v)$ to be a solution of the stationary Fokker-Planck equation whose general form is

$$\frac{\partial}{\partial v} [a(v)f(v)] = \frac{1}{2} \frac{\partial^2}{\partial v^2} [\sigma^2(v)f(v)] , \tag{46}$$

when the time derivative of $f(v)$ is small enough to be ignored, as in the quasi-equilibrium evolution we consider here. In gravitating systems, the high-velocity limits of the functions $a(v)$ and $\sigma^2(v)$ which characterize dynamical friction and stochastic acceleration have the form (e.g., Saslaw 1985*a*)

$$a(v) = -\delta v^2; \qquad \sigma^2(v) = \gamma v^{-3} , \tag{47}$$

where δ and γ are positive constants.

Substituting these gravitational functions into equation (46) and retaining only the dominant terms for large v gives the simple result

$$\frac{df}{dv} = -2\frac{\delta}{\gamma} vf , \tag{48}$$

which is identical to equation (45) if we identify

$$\frac{\delta}{\gamma} = -\alpha \ln (be^{1-b}) , \tag{49}$$

which is consistent with their gravitational form at large v. Thus, the asymptotic form of $f(v)$ satisfies the gravitational Fokker-Planck equation, as expected, with a tail which is essentially Maxwellian.

c) *Comparison with N-Body Experiments*

We can test the $f(v)$ distribution derived here by comparing it with N-body simulations. Eventually, when accurate secondary distance indicators are known for an extensive fair sample of galaxies (see e.g., Sandage and Bedke 1988 for a large summary of this problem) it will also be possible to observe $f(v)$ and determine whether the actual peculiar velocities of galaxies, like their positions, are consistent with gravitational clustering. If so, the absolute values of the observed peculiar radial velocities should have the distribution of equation (42).

To compare the theoretical distribution of equation (42) with N-body simulations, we analyze further the gravitational experiments whose spatial distributions were examined earlier by Itoh *et al.* (1988). Here we investigate their velocity distributions. These experiments used a vectorized direct integration technique (Aarseth code) to follow the motion of 4000 galaxies in expanding universes with various initial conditions and values of the density parameters Ω_0. The cases we explore here are for $\Omega_0 = 1$, 0.1, and 0.01 with initial Poisson distributions which begin cold with no motion relative to the Hubble flow.

The comparisons are shown in Figures 1–3 for $\Omega_0 = 1$, 0.1, and 0.01, respectively. Each figure shows four comparisons, at different expansion factors a/a_0 with $a_0 = 1$ initially. The solid histogram is the experimental distribution; the light dashed line to the right of each histogram is a Maxwell-Boltzmann distribution with the same velocity dispersion as the data and is shown just for illustration; the heavy dashed line is a least-squares fit of the theoretical distribution of equation (42) to the experimental histogram. In the fit, the quantities b, α, and β were considered as free parameters whose fitted values can then be compared with their values measured directly from the data.

The precision of these fits is surprising. They show that the form of equation (42) does indeed provide a very good description of the velocity distribution. Since β is determined by the overall velocity dispersion, α is given by equation (41) and b is known from the spatial distribution, there are, in principle, no free parameters in the theory (although it does not take the distribution of α and b around their average values into account).

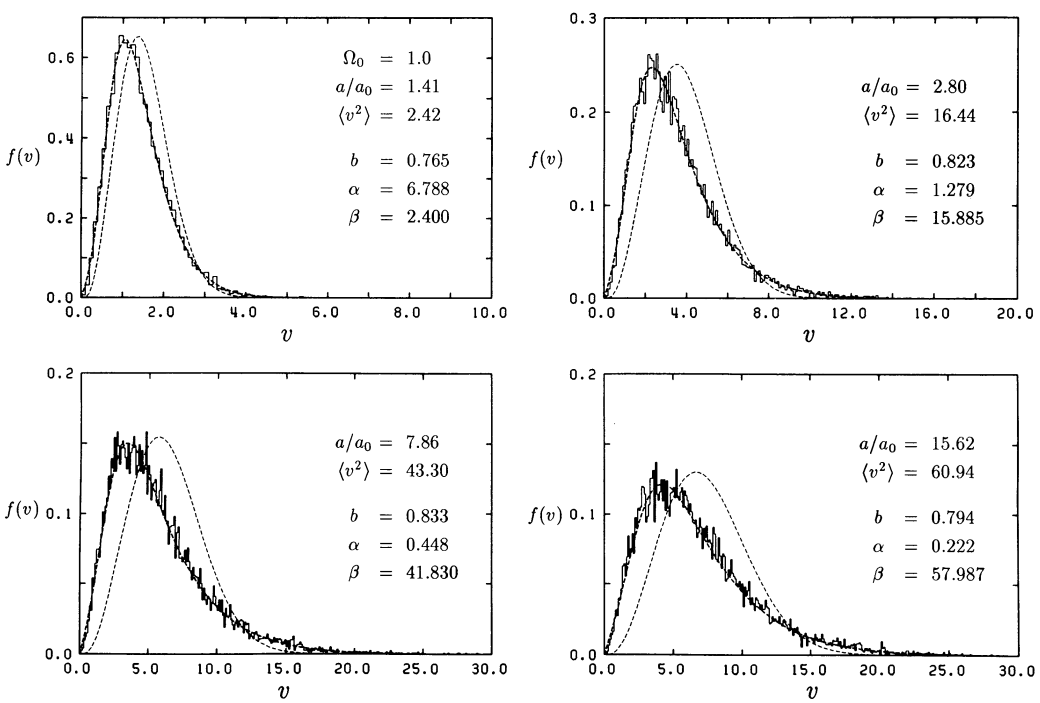

FIG. 1.—Velocity distributions averaged over the four $\Omega_0 = 1.0$ simulations. Each panel shows a different epoch a/a_0. The light dashed line to the right of each experimental histogram is a comparison Maxwell-Boltzmann distribution with the same velocity dispersion, $\langle v^2 \rangle$, as the simulation. The heavier dashed line through each histogram is the best fit to the gravitational quasi-equilibrium velocity distribution of eq. (42). The comoving velocity would be v/a.

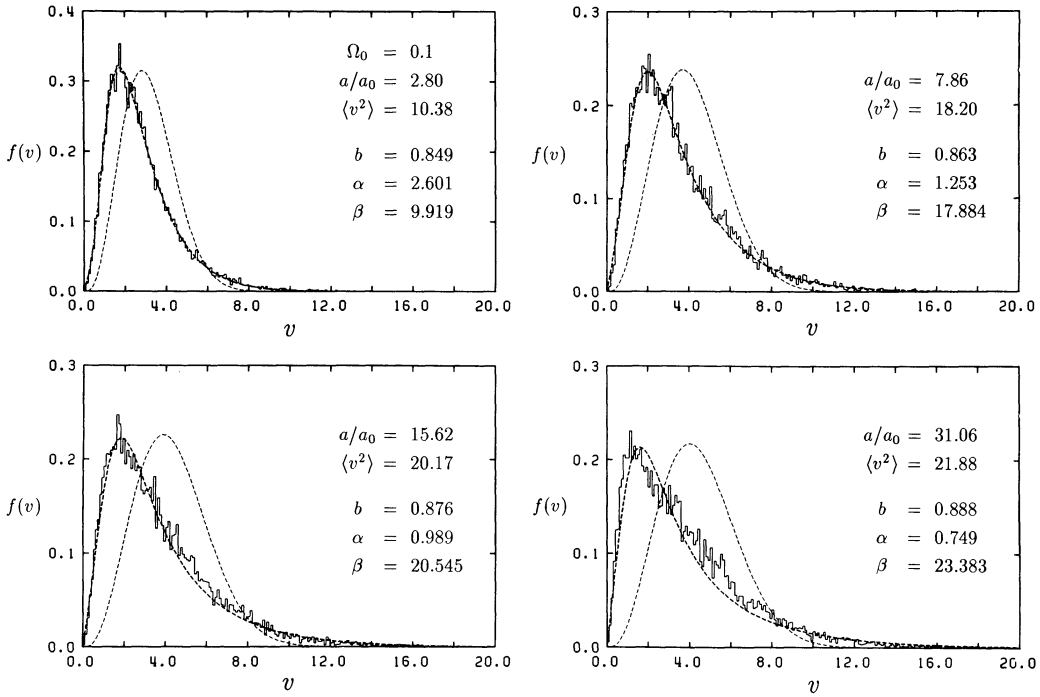

FIG. 2.—Velocity distributions averaged over the four $\Omega_0 = 0.1$ simulations. Each panel shows a different epoch a/a_0. The light dashed line to the right of each experimental histogram is a comparison Maxwell-Boltzmann distribution with the same velocity dispersion, $\langle v^2 \rangle$, as the simulation. The heavier dashed line through each histogram is the best fit to the gravitational quasi-equilibrium velocity distribution of eq. (42).

Tables 1*a*–1*c* give the best least-squares fits of b, α, and β for various expansion factors, as well as giving the average velocity dispersion measured directly from the galaxy velocities in the experiment. These are averaged over four simulations for each value of Ω_0. The agreement between β and $\langle v^2 \rangle$ is remarkable (better than $\sim 4\%$) when $\Omega_0 = 1$, which is the most relaxed quasi-equilibrium case. This specifically confirms equation (43). Agreement is still very good when $\Omega_0 = 0.1$, but it becomes rather poor for the $\Omega_0 = 0.01$ model which, as the complementary spatial distributions in Itoh *et al.* (1988) show, is far from quasi-equilibrium. A similar trend is apparent in the vaues of b. For $\Omega_0 = 1$, the value of b for $f(v)$ is in good agreement with the value determined for $f(N)$

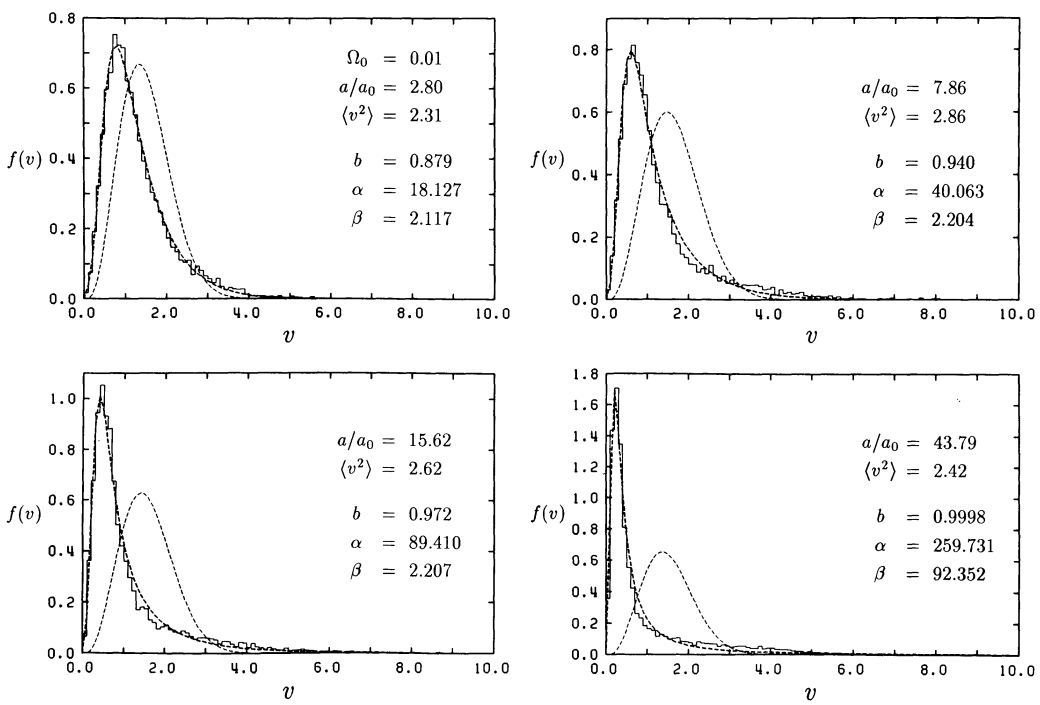

FIG. 3.—Velocity distributions averaged over the four $\Omega_0 = 0.01$ simulations. Each panel shows a different epoch a/a_0. The light dashed line to the right of each experimental histogram is a comparison Maxwell-Boltzmann distribution with the same velocity dispersion, $\langle v^2 \rangle$, as the simulation. The heavier dashed line through each histogram is the best fit to the gravitational quasi-equilibrium velocity distribution of eq. (42).

TABLE 1*a*

BEST-FIT PARAMETERS FOR THE SIMULATIONS WITH $\Omega_0 = 1$

a/a_0	b	α	β	$\langle v^2 \rangle$
1.41.....	0.7652	6.7883	2.4001	2.42
1.99.....	0.8275	2.6579	8.7799	8.84
2.80.....	0.8229	1.2791	15.8851	16.44
3.95.....	0.8482	1.0775	23.6628	24.11
5.57.....	0.8333	0.6498	31.5735	32.50
7.86.....	0.8327	0.4482	41.8303	43.30
11.08.....	0.8322	0.3570	50.0164	50.92
15.62.....	0.7938	0.2216	57.9872	60.94

TABLE 1*b*

BEST-FIT PARAMETERS FOR THE SIMULATIONS WITH $\Omega_0 = 0.1$

a/a_0	b	α	β	$\langle v^2 \rangle$
1.41.....	0.7539	8.4445	1.7393	1.77
1.99.....	0.8326	3.9765	5.9632	6.08
2.80.....	0.8491	2.6007	9.9189	10.38
3.95.....	0.8679	2.2080	13.3451	13.66
5.57.....	0.8689	1.7743	15.2695	15.96
7.86.....	0.8630	1.2529	17.8835	18.20
11.08.....	0.8695	1.0458	19.7958	19.77
15.62.....	0.8758	0.9893	20.5446	20.17
22.03.....	0.8682	0.7786	21.0638	21.13
31.06.....	0.8875	0.7488	23.3825	21.88

TABLE 1*c*

BEST-FIT PARAMETERS FOR THE SIMULATIONS WITH $\Omega_0 = 0.01$

a/a_0	b	α	β	$\langle v^2 \rangle$
1.41.....	0.7480	28.2310	0.5139	0.51
1.99.....	0.8225	16.8569	1.3841	1.39
2.80.....	0.8788	18.1274	2.1173	2.31
3.95.....	0.8921	19.0976	2.2681	2.80
5.57.....	0.9161	25.2818	2.2963	2.79
7.86.....	0.9395	40.0631	2.2036	2.86
11.08.....	0.9594	59.3671	2.2662	2.76
15.62.....	0.9719	89.4095	2.2071	2.62
22.03.....	0.9873	147.2626	3.0622	2.53
31.06.....	0.9960	246.3054	6.0964	2.49
43.79.....	0.9998	259.7312	92.3521	2.42

(Fig. 8 of Itoh *et al.* 1988) after the system has relaxed. Interestingly, the value of b obtained from the velocity distribution rises to this relaxed value much faster than the value determined from the spatial distribution. This is expected, because the peculiar velocities must build up before the galaxies are able to move into their more correlated positions. This effect increases as Ω_0 decreases and the velocity dispersions become smaller. It is especially evident for $\Omega_0 = 0.01$, where it is reflected in the high values of $b_{\text{ab initio}}$ in Figure 8 of Itoh *et al.* (1988), compared with the small corresponding values of b_{fit} for those spatial distributions. This lack of relaxation for small Ω_0 can also be seen in the poorer fit to the tails of those $f(v)$ distributions in our Figure 3.

Comparison of the gravitational velocity distribution $f(v)$ with the Maxwellian having the same $\langle v^2 \rangle$ in Figures 1–3 is also rather interesting. In all cases, the gravitational distribution has a colder peak than its associated Maxwellian, and the relative difference between their peaks increases as the universe expands. This is a symptom of clustering. Lower density unbound regions, which predominate, lose energy to the expansion of the universe and cool relative to a Maxwellian distribution. Universes with smaller values of Ω_0 have more field galaxies. So this difference between $f(v)$ and a Maxwellian should increase as Ω_0 decreases, as Figures 1–3 show it does. The higher tail of $f(v)$ relative to the Maxwellian is caused by the small number of strongly bound clusters, which nonetheless contain a significant fraction of all galaxies, and which do not lose appreciable internal energy to the general expansion. This becomes especially apparent for $\Omega_0 = 0.01$, where the overall distribution is very cold with a small number of bound clusters, forming a warm-velocity tail which far exceeds the Maxwellian value and somewhat exceeds the gravitational distribution. Even in this $\Omega_0 = 0.01$ case, however, the bulk of the velocities fit the form of the gravitational distribution very well, although their values of α and β cannot be represented by overall averages and indicate an expansion away from the quasi-equilibrium state.

We next consider the value of α in more detail, first asking how well its average determined by $f(v)$ satisfies equation (41). The average inverse radius for a uniform Poisson distribution is given by (e.g., Saslaw 1985*a* equation 33.23 with $a = 0$)

$$\left\langle \frac{1}{r} \right\rangle = N^{1/3}\Gamma\left(\frac{2}{3}\right) = 1.35N^{1/3} = 21.4\,, \tag{50}$$

where the last expression is for the $N = 4000$ particles used in our simulation whose total radius is normalized to unity. Thus, we expect $\alpha\beta = 21.4$. From Table 1*a* for $\Omega_0 = 1.0$ the values of $\alpha\beta$ at the eight successive expansion radii are, respectively, 16.3, 23.4, 20.7, 25.5, 20.5, 18.7, 17.9, and 12.8. The average of all these values is $\langle\alpha\beta\rangle_{1-8} = 19.5$, and the average, omitting the first and last values (which may not be in quasi-equilibrium), is $\langle\alpha\beta\rangle_{2-7} = 21.1$. These are in reasonable agreement with equation (50), even though individual values may fluctuate significantly. If we were to use the values of $\langle v^2\rangle$ measured directly from the data, rather than the fitted values of β, the agreement of $\alpha\langle v^2\rangle$ with equation (50) would be slightly better: 19.9 for all values and 21.5 omitting the first and last. In the case $\Omega_0 = 0.1$ from Table 1*b* we find $\langle\alpha\beta\rangle_{2-9} = 23.2$ and $\langle\alpha\beta\rangle_{1-10} = 21.8$. In this case, the average of $\alpha\langle v^2\rangle$ directly from all the data values is 22.1. Omitting the first and last, the average is 23.7, so these values are again close to equation (50). A glance at Table 1*c*, however, shows strong disagreement between the values of $\alpha\beta$ or $\alpha\langle v^2\rangle$ and the expected value from equation (50) in the case of $\Omega_0 = 0.01$. This is caused by the gross departure from quasi-equilibrium for low Ω_0. These distributions separate into a very cold Hubble flow involving most of the galaxies and a few compact clusters. Referring back to the discussion following equation (40), we see that large values of α indicate that most of the distribution is uncondensed, and for $\Omega_0 = 0.01$ the value of α generally increases rapidly with expansion. By contrast, for $\Omega_0 = 1.0$ and 0.1, the values of α decrease with the expansion, indicating that clustering becomes stronger. Indeed, α seems to be a good way to measure how the state of clustering evolves.

We can go further and explore how α fluctuates from place to place, at any given time. We illustrate this for the four $\Omega_0 = 1.0$ simulations, since they are closest to quasi-equilibrium. The two upper panels of Figure 4 show the peculiar velocity dispersions in spheres containing a given number, N, of galaxies at the two expansion epochs $a/a_0 = 2.8$ and 7.86, respectively. These diagrams are obtained by first choosing 25 random spatial points within a radius $R = 0.6$ of the center of each simulation. Then we find the N nearest galaxies to each random point and calculate the velocity dispersion of their peculiar motions. This is plotted for every twentieth value of N. Results for each of the four simulations start at values of $N = 20$, 25, 30, and 35, respectively, for clarity. Thus, for each value of N in the upper panels, every point represents the velocity dispersion in a sample sphere containing N galaxies. The dashed horizontal line shows the average velocity dispersion within $R = 0.8$ for the entire example.

Initially the galaxies move just with the Hubble expansion and $v_N^2 = 0$ for all N. The velocity dispersion builds up very rapidly, particularly for small groups which form quickly. Large values of N automatically average over the velocities of many weakly clustered galaxies, thus giving a lower and more representative value of v_N^2. At later times, interesting network patterns develop in the individual diagrams. They portray the correlations between velocity dispersion and spatial clustering. Figure 5 shows an example at higher resolution for a single simulation. The thick streaks whose v_N^2 decreases with increasing N arise from the random spatial points which happen to fall near the centers of strongly bound clusters where the velocity dispersion is large. It decreases toward the average with increasing distance from the cluster as more loosely bound and "field" galaxies are counted. The thin chains whose v_N^2 increases with increasing N arise from spatial points outside the cores of strong clusters, but whose spatial sphere begins to encompass a core as N increases. The points at small N with very low v_N^2 are those which happen to be in underdense regions. So this provides a rather nice pictorial representation of both position and velocity clustering, which could eventually be compared with observations.

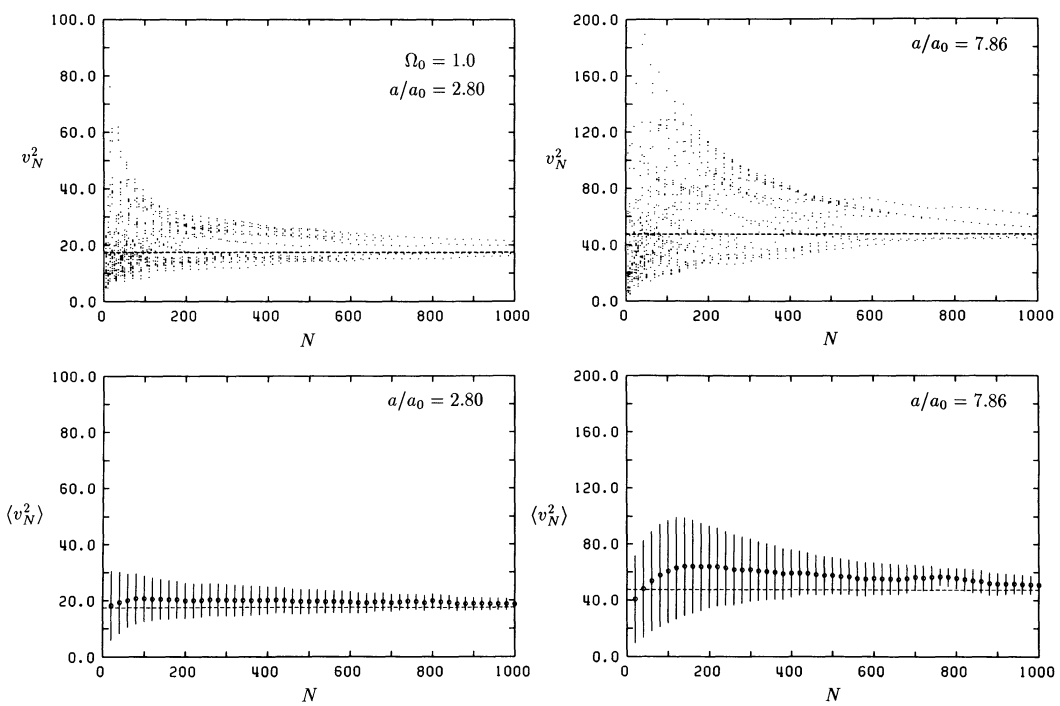

FIG. 4.—Velocity dispersions, v_N^2, in spheres with a given number of galaxies for four $\Omega_0 = 1$ simulations, shown at expansion epochs of 2.8 and 7.86. Points in the upper two panels are values around 25 randomly selected points within $R = 0.6$ for each simulation. For clarity, the values of N plotted are $N = 20$, 40, 60, etc., for the first simulation, $N = 25$, 45, 65, etc., for the second, and so on. The horizontal dashed line is the average velocity dispersion of all galaxies within $R = 0.8$. The lower two panels give the average and standard deviation for all spheres of a given N.

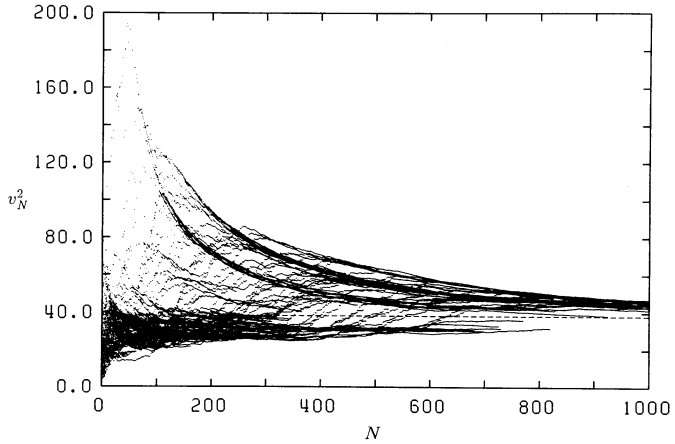

FIG. 5.—A higher resolution version of the upper right panel of Fig. 4 at $a/a_0 = 7.86$. This is for one $\Omega_0 = 1$ simulation with spheres of different N around 100 points selected randomly throughout the entire simulation. Each value of N is plotted. All 4000 particles are used.

The two lower panels of Figure 4 give the average and the standard deviation of v_N^2 for each value of N in the upper panels. For values of N between about 20 and 100, the average value of v_N^2 increases reasonably linearly with N. For large N, it reaches an average value close to that of all the galaxies within $R = 0.8$. Larger values of N typically sample regions containing several clusters and many field galaxies, so as N increases they become more representative of the entire system. The linear increase of v_N^2 with N is consistent with our assumption in equation (40) of an average value of α. The standard deviation of α in different regions is indicated by the vertical bars. However, most regions have a smaller range of α than these suggest, because the standard deviations are increased by a few strongly bound groups with high-velocity dispersions, as the upper panels and Figure 5 show. Thus, although there is a significant range of α in regions having the same number of galaxies, using an average value for α seems to provide a good approximation for the velocity distribution.

We examine the nature of α from another point of view in Figure 6. Here we have chosen spheres of given radii, $R = 0.02$, 0.04, 0.06, 0.08, 0.1, 0.2, 0.3, and 0.4, around 9500 random spatial points in each of the same four $\Omega_0 = 1$ simulations. The values of N and the velocity dispersion $\langle v_R^2 \rangle$ for each of these spheres give the overall averages and standard deviations for $\langle v_R^2 \rangle$. As the system evolves, there is again an increasing absolute dispersion around the average value of $\langle v_R^2 \rangle$, especially for small values of R. Despite this scatter, one sees a fairly linear relation between $\langle v_R^2 \rangle$ and N, again most clearly for small values of R and N. For $R \geq 0.3$, this linear relation seems to have a break at larger values of N. Moreover, the slope, which is the value of α, differs for the different radii.

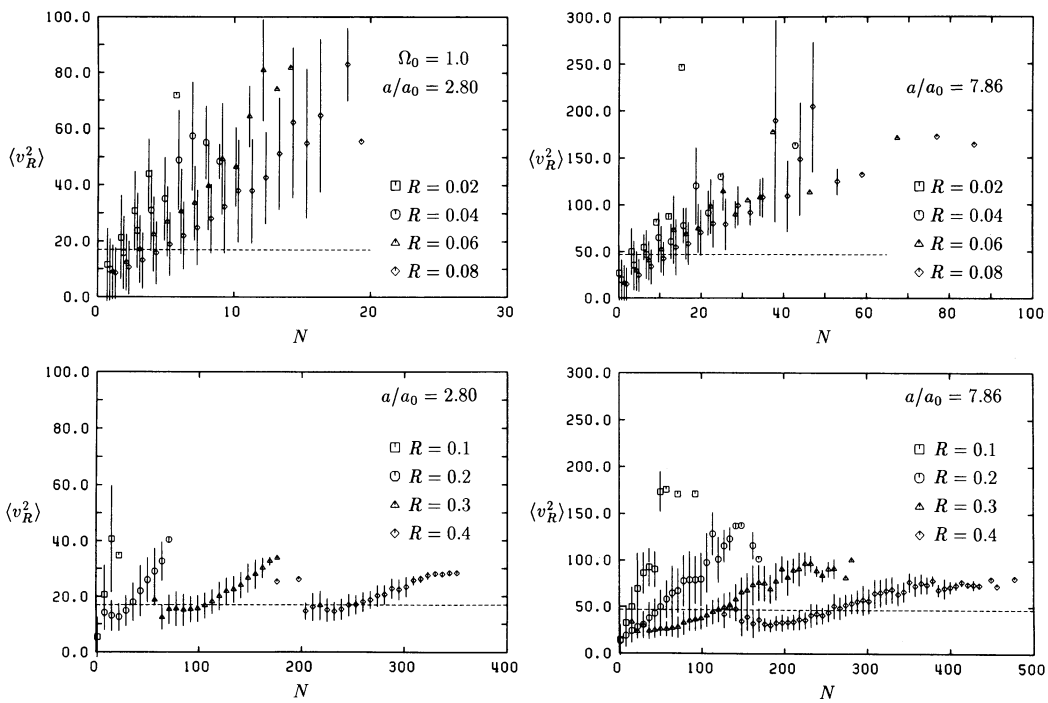

FIG. 6.—Velocity dispersions in spheres of given radius, averaged over four $\Omega_0 = 1$ simulations, shown at expansion epochs 2.8 and 7.86. Radii of spheres range from 0.02 to 0.4.

Therefore, the average value of α determined by equation (41) must represent a weighted average over these different radii. The procedure for weighing this average is not clear and would be a useful development of our theory. Meanwhile, we rely on the agreement between $f(v)$ in equation (42) and the computer experiments.

V. DISCUSSION

The discovery of the velocity distribution $f(v)$, combined with the previously known number distribution $f(N)$, now provides a complete description of quasi-equilibrium gravitational clustering in the expanding universe at the same level as the Maxwell-Boltzmann description of equilibrium in a perfect gas. Unlike the Maxwell-Boltzmann case, the gravitational distribution functions show the strong effects of correlations induced by the gravitational forces: density fluctuations are correlated among themselves, velocity fluctuations are correlated among themselves, and density fluctuations are correlated with velocity fluctuations. The distribution functions implicitly include the effects of these correlations to all orders. That is why they are in such good agreement with the N-body computer simulations of quasi-equilibrium evolution.

Like the Maxwell-Boltzmann distribution, which can be derived from just the assumptions of translational and rotational invariance (homogeneity and isotropy), the quasi-equilibrium gravitational distribution in an expanding universe can be derived from simple fundamental assumptions. For the spatial distribution $f(N)$ these assumptions are statistical homogeneity, scale invariance, the Poisson limit for very large N, and of course the pairwise nature of the gravitational potential. For the velocity distribution $f(v)$, the assumptions are that the combined distribution function $f(N, v)$ separates into $f(N)f(v)$ in quasi-equilibrium and that the kinetic energy fluctuations are, on average, proportional to the potential energy fluctuations. It is probably possible to refine this last assumption to take into account the result, shown by our numerical experiments, that the proportionality between these energy fluctuations itself varies from place to place. Even without this refinement, however, the experiments show excellent fits to the theoretical $f(v)$ with no free parameters. Whether the observed galaxy distribution also fits $f(v)$, as it does $f(N)$, is a matter for future observations to decide.

We have also developed the early stages of a nonequilibrium kinetic theory which shows explicitly how the gravitational system evolves away from its initial uncorrelated state toward the observed $f(N)$ distribution for galaxies. This is done quite simply by relating the explicit generating function of the $f(N)$ distribution to the BBGKY hierarchy of correlation functions. This ties the evolution of $f(N)$ into standard kinetic theory. One consequence is a value for the amplitude of the three-point correlation function, which is consistent with the observed value for galaxy clustering.

These new links between the density distribution, the velocity distribution, and kinetic theory appear to have considerable potential for a broader and more profound understanding of gravitational galaxy clustering in our expanding universe.

S. M. Chitre and S. Inagaki thank the Virginia Institute of Theoretical Astrophysics and the Astronomy Department of the University of Virginia for their support and hospitality. S. M. Chitre thanks the National Science Foundation for travel support under INDO-US grant No. INT 87-15411. S. Inagaki and M. Itoh thank the Yamada Science Foundation for partial support. The numerical calculations were done at the Kyoto University Data Processing Center.

REFERENCES

Balian, R., and Schaeffer, R. 1989, *Astr. Ap.*, **220**, 1.
Coleman, P. H., Pietronero, L., and Sanders, R. H. 1988, *Astr. Ap.* (*Letters*), **302**, L1.
Coleman, P., and Saslaw, W. C. 1990, *Ap. J.*, **353**, 354.
Crane, P., and Saslaw, W. C. 1986, *Ap. J.*, **301**, 1.
———. 1988, in *Dark Matter*, ed. J. Adouze and J. Tran ThanhVan (Gif-sur-Yvette: Editions Frontiers), p. 171.
Gott, J. R., *et al.* 1989, *Ap. J.*, **340**, 625.
Groth, E. J., and Peebles, P. J. E. 1977, *Ap. J.*, **217**, 385.
Herschel, W. 1785, *Phil. Trans. Roy. Soc. London*, *A* **75**, 213.
Itoh, M., Inagaki, S., and Saslaw, W. C. 1988, *Ap. J.*, **331**, 45.
———. 1990, *Ap. J.*, **356**, 315.
Landau, L. D., and Lifshitz, E. M. 1958, *Statistical Physics* (New York: Addison Wesley).
Peebles, P. J. E. 1980, *The Large Scale Structure of the Universe* (Princeton: Princeton University Press).
Pietronero, L. 1987, *Physica*, **144A**, 257.
Sandage, A., and Bedke, J. 1988, *Atlas of Galaxies Useful for Measuring the Cosmological Distance Scale* (Washington, DC: NASA).
Saslaw, W. C. 1985*a*, *Gravitational Physics of Stellar and Galactic Systems* (Cambridge: Cambridge University Press).
———. 1985*b*, *Ap. J.*, **297**, 49.
———. 1986, *Ap. J.*, **304**, 11.
———. 1989, *Ap. J.*, **341**, 588.
Saslaw, W. C., and Hamilton, A. J. S. 1984, *Ap. J.*, **276**, 13.
Suto, Y., Itoh, M., and Inagaki, S. 1990, *Ap. J.*, **350**, 492.
Zhan, Y. 1989, *Ap. J.*, **340**, 23.
Zhan, Y., and Dyer, C. 1989, *Ap. J.*, **343**, 107.

S. M. Chitre: Tata Institute of Fundamental Research, Homi Bhabha Road, Bombay 400 005, India

Shogo Inagaki and Makoto Itoh: Department of Astronomy, University of Kyoto, Kyoto 606, Japan

William C. Saslaw: Department of Astronomy, University of Virginia, P.O. Box, 3818, University Station, Charlottesville, VA 22903-0818